

# Vibrational Circular Dichroism in Transition-Metal Complexes. 4. Solution Conformation of $\Lambda$ -*mer*- and $\Lambda$ -*fac*-Tris( $\beta$ -alaninato)cobalt(III)

Daryl A. Young, Teresa B. Freedman,\* and Laurence A. Nafie\*

Contribution from the Department of Chemistry, Syracuse University, Syracuse, New York 13244-1200. Received April 24, 1987

**Abstract:** The CH stretching absorption and vibrational circular dichroism (VCD) spectra of  $\Lambda$ -*mer*- and  $\Lambda$ -*fac*-tris( $\beta$ -alaninato)cobalt(III) in D<sub>2</sub>O solution are reported. Enhanced VCD features are observed for the out-of-phase ("B") antisymmetric and symmetric CH<sub>2</sub> stretches of the two methylene groups, whereas little or no VCD intensity is observed for the in-phase ("A") modes. The VCD bands for the facial complex are three times as intense as those for the meridional complex. The VCD enhancement is interpreted in terms of ring current generated around the ligand ring by the concerted out-of-phase oscillation of the equatorial CH bonds. The sense of twist found for the two methylene groups in each ring of the  $\Lambda$ -facial complex corresponds to the  $\delta$  conformation of ethylenediamine. In the  $\Lambda$ -meridional complex one ring has the opposite sense of twist. The ring conformations deduced from the VCD spectra are similar to those reported for the crystalline meridional complex.

Vibrational circular dichroism (VCD)<sup>1-4</sup> spectroscopy has been shown to be a valuable technique for determining the solution conformation of chiral transition-metal chelate complexes.<sup>5-7</sup> The sign of a VCD feature arises from the relative orientations of the electric and magnetic dipole transition moments for the vibrational mode. If the directions of these moments can be deduced for a variety of ring conformations, correlation of the predicted and observed VCD intensities leads to a limited range of possible solution geometries. For CH stretching modes, the direction of the electric dipole transition moment is readily obtained by finding the resultant of vectors located on the CH oscillators, which are directed C  $\rightarrow$  H for bond contraction and H  $\rightarrow$  C for elongation<sup>8</sup> and have lengths proportional to the bond displacement. The magnetic dipole transition moment can arise from two main mechanisms. The coupled oscillator mechanism<sup>9</sup> for in- and out-of-phase coupled motion of two oscillators within a single ring or exciton coupling among vibrations on different chelate rings results in a conservative bisignate VCD couplet for each type of coupled motion. Such features have not been observed in the CH stretching VCD spectra of the 5-membered chelate rings (amino acid<sup>7</sup> and ethylenediamine ligands<sup>6</sup>) thus far investigated. The intense monosignate VCD features in these complexes can be interpreted in terms of the ring current mechanism for VCD.<sup>1,5-7,10,11</sup> According to this mechanism, the magnetic dipole transition moment results from an electronic current oscillating in the closed ring, which is generated by the CH stretching motions. Three empirical rules have been devised for determining the sense of ring current for a given phase of vibrational motion, from which the direction of the ring current magnetic dipole transition moment can be deduced.<sup>1,6,11</sup>

In our analysis of the CH stretching VCD spectra of the ethylenediamine complexes,<sup>6</sup> we attributed the VCD intensity to ring current generated by the motion of the equatorial CH bonds

**Table I.** Frequencies, Intensities, and Assignments of the CH Stretching Absorption and VCD Spectra of Tris( $\beta$ -alaninato)cobalt(III) Complexes in D<sub>2</sub>O

absorption		VCD		
freq, cm <sup>-1</sup>	$\epsilon$ , 10 <sup>3</sup> cm <sup>2</sup> mol <sup>-1</sup> obsd (calcd) <sup>b</sup>	freq, cm <sup>-1</sup>	10 <sup>3</sup> $\Delta\epsilon$ , 10 <sup>3</sup> cm <sup>2</sup> mol <sup>-1</sup> obsd (calcd) <sup>b</sup>	assignment <sup>a</sup>
$\Lambda$ - <i>fac</i> -Co( $\beta$ -ala) <sub>3</sub>				
2977	34 (34)	2978	+4.8 (-1.4)	$\nu$ (CH <sub>2</sub> ) <sup>asym</sup> "B"
2958	29 (27)		(+2.6)	$\nu$ (CH <sub>2</sub> ) <sup>asym</sup> "A"
2936	25 (12)	2934	-4.3 (+0.5)	$\nu$ (CH <sub>2</sub> ) <sup>sym</sup> "B"
2908	32 (15)		(-1.8)	$\nu$ (CH <sub>2</sub> ) <sup>sym</sup> "A"
$\Lambda$ - <i>mer</i> -Co( $\beta$ -ala) <sub>3</sub>				
2980	31	2978	+1.5	$\nu$ (CH <sub>2</sub> ) <sup>asym</sup> "B"
2960	26			$\nu$ (CH <sub>2</sub> ) <sup>asym</sup> "A"
2936	18	2940	-1.1	$\nu$ (CH <sub>2</sub> ) <sup>sym</sup> "B"
2905	26			$\nu$ (CH <sub>2</sub> ) <sup>sym</sup> "A"

<sup>a</sup> asym = antisymmetric; sym = symmetric; "B" = mode is antisymmetric with respect to pseudo-C<sub>2</sub> axis perpendicular to methylene CC bond; "A" = mode is symmetric with respect to rotation about the pseudo-C<sub>2</sub> axis. <sup>b</sup> Fixed partial charge calculations for the ND<sub>2</sub>C(1)-H<sub>2</sub>C(2)H<sub>2</sub>C group in conformation **1** with 60° dihedral angle. Charges scaled to fit absorption intensity at 2977 cm<sup>-1</sup>.

in the out-of-phase (B symmetry) combination of the antisymmetric or symmetric stretches of the two methylene groups. The in-phase (A symmetry) modes cannot generate ring current. However, since the A and B modes were not resolved in the CH stretching spectra of the ethylenediamine complexes, the presence of any VCD intensity due to the A modes or to the coupled oscillator mechanism could not be ascertained. In the six-membered  $\beta$ -alanine ligand ring, OCoNCH<sub>2</sub>CH<sub>2</sub>C=O, the two methylene groups can assume orientations corresponding to the  $\lambda$  and  $\delta$  configurations of the ethylenediamine ring,<sup>12</sup> and because the methylene groups are in nonequivalent environments, the frequencies of the pseudo "A" and "B" stretching modes should be separated. In order to provide further insight into the mechanisms for generating VCD intensity in transition-metal complexes and to extend our studies to six-membered chelate rings, we have investigated the CH stretching VCD in  $\Lambda$ -*fac*- and  $\Lambda$ -*mer*-tris( $\beta$ -alaninato)cobalt(II).

## Experimental Section

Tris( $\beta$ -alaninato)cobalt(III) was prepared<sup>13</sup> by heating a solution of  $\beta$ -alanine and hexamminecobalt(III) in the presence of potassium hy-

(1) Freedman, T. B.; Nafie, L. A. In *Topics in Stereochemistry*; Eliel, E., Wilen, S., Eds.; Wiley: New York, 1987; Vol. 17, pp 113-206.

(2) Stephens, P. J.; Lowe, M. A. *Annu. Rev. Phys. Chem.* **1985**, *36*, 213.

(3) Keiderling, T. A. *Appl. Spectrosc. Rev.* **1981**, *17*, 189.

(4) Nafie, L. A. In *Advances in Infrared and Raman Spectroscopy*; Clark, R. J. M., Hester, R. E., Eds.; Wiley-Heyden: London, 1984; Vol. II, p 49.

(5) Young, D. A.; Lipp, E. D.; Nafie, L. A. *J. Am. Chem. Soc.* **1985**, *107*, 6205.

(6) Young, D. A.; Freedman, T. B.; Lipp, E. D.; Nafie, L. A. *J. Am. Chem. Soc.* **1986**, *108*, 7255.

(7) Freedman, T. B.; Young, D. A.; Oboodi, M. R.; Nafie, L. A. *J. Am. Chem. Soc.* **1987**, *109*, 1551.

(8) Wiberg, K. B.; Wendoloski, J. J. *J. Phys. Chem.* **1984**, *88*, 586.

(9) (a) Holzwarth, G.; Chabay, I. *J. Chem. Phys.* **1972**, *57*, 1632. (b) Sugeta, H.; Marcott, C.; Faulkner, T. R.; Overend, J.; Moscovitz, A. *Chem. Phys. Lett.* **1976**, *40*, 397.

(10) Nafie, L. A.; Freedman, T. B. *J. Phys. Chem.* **1986**, *90*, 763.

(11) Freedman, T. B.; Balukjian, G. A.; Nafie, L. A. *J. Am. Chem. Soc.* **1985**, *107*, 6213.

(12) Mason, S. F. In *Optical Rotatory Dispersion and Circular Dichroism*; Ciardelli, F., Salvadori, P., Eds.; Heyden: London, 1973; pp 196-237.

(13) Celap, M. B.; Niketic, S. R.; Janjic, T. J.; Nikolic, Y. N. *Inorg. Chem.* **1967**, *6*, 2063.

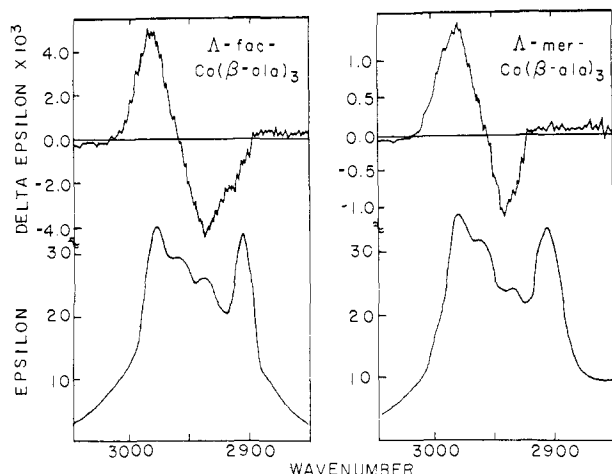


**Figure 1.** CH stretching absorption (lower traces) and VCD (upper traces) spectra of tris( $\beta$ -alaninato)cobalt(III) complexes in  $D_2O$  solution.  $\Delta$ -*fac*-Co( $\beta$ -ala) $_3$ : 0.052 M, 200  $\mu$ m path length,  $\Delta$ -*mer*-Co( $\beta$ -ala) $_3$ : 0.17 M, 200  $\mu$ m path length.

dioxide. The hexamminecobalt(III) was synthesized by the air oxidation of a solution of cobalt(II) chloride, ammonium chloride, and ammonia.<sup>14</sup> The meridional and facial isomers were separated on the basis of solubility differences. The racemic mixtures of *mer*- and *fac*-Co( $\beta$ -ala) $_3$  were resolved by chromatographic separation on a QUA-Sephadex A-25 anion exchange column loaded with antimony D-tartrate as the resolving agent.<sup>15</sup> The identity of each complex was confirmed by visible absorption, electronic circular dichroism, and infrared spectra.

In order to remove interference from the intense NH stretching modes, the amine groups were deuterated by exchange in  $D_2O$ . Spectra were obtained for  $D_2O$  solutions in a variable path length cell equipped with  $CaF_2$  windows.

Infrared spectra were obtained at 4-cm<sup>-1</sup> resolution on a Nicolet 7199 FTIR spectrometer.  $D_2O$  background absorptions were removed by spectral subtraction. The VCD spectra were measured at 12 cm<sup>-1</sup> on a dispersive VCD spectrometer described previously.<sup>16</sup> The average VCD spectrum of the two enantiomers was used for the VCD base line for each complex.

## Results

The CH stretching absorption and VCD spectra of  $\Delta$ -*fac*- and  $\Delta$ -*mer*-tris( $\beta$ -alaninato)cobalt(III) are presented in Figure 1. The band frequencies, intensities, and assignments are compiled in Table I. The absorption spectra of the two complexes, consisting of four distinct features, are quite similar in both frequency and intensity. We assign the two higher frequency bands to the coupled antisymmetric stretching modes of the two methylene groups and the two lower frequency bands to the coupled symmetric stretches. The modes in each region are split in frequency since the two methylene groups in a ring are nonequivalent. For ethylenediamine ligands only a single band is observed in each CH stretching region.<sup>6</sup> For each  $\beta$ -alaninato complex, the positive VCD band corresponds to the higher frequency antisymmetric stretching mode and the negative VCD feature corresponds to the higher frequency symmetric stretching mode, whereas little or no VCD intensity arises for the other two modes. The VCD intensities for the facial complex are approximately three times larger than those observed for the meridional complex.

We can further characterize the stretching modes in the complexes by considering the relative intensities predicted for the coupled methylene modes as a function of torsion angle. In Figure

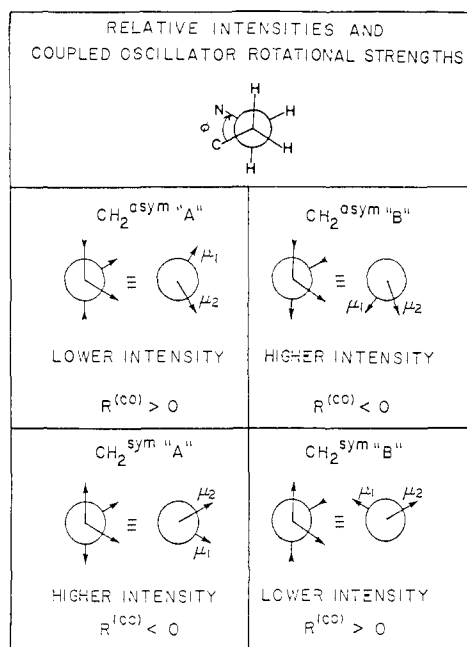


**Figure 2.** Coupled CH stretching motions for adjacent methylene groups in the Co( $\beta$ -ala) ring with NCCC dihedral angle  $+60^\circ$ . "A" and "B" symmetry designations refer to displacements that are respectively symmetric and antisymmetric to rotation about a pseudo- $C_2$  axis orthogonal to the C-C bond between the methylene groups. For each mode, the Newman diagram to the left shows relative CH bond displacements; the Newman projection to the right shows relative orientations of electric dipole transition moments for the two methylene groups. Absorption intensity for each mode is proportional to the absolute square of the vector sum of the two transition moments.  $R^{(CO)}$  is the rotational strength resulting from the coupled oscillator mechanism for the two electric dipole transition moments.

2 we show Newman projections of the four stretching modes for a  $+60^\circ$  dihedral angle  $\phi$  between the two methylenes, assuming equal contributions from the two groups. For each mode, the Newman projection to the left shows the relative bond motions (CH elongation or contraction) and the Newman projection to the right gives the relative orientations of the net electric dipole transition moments for each methylene group. The modes are labeled by their symmetry with respect to rotation about the pseudo- $C_2$  axis perpendicular to the C-C bond between the methylene groups. As a result of the net dipole orientations, for a torsion angle range  $-90^\circ < \phi < +90^\circ$ , in the antisymmetric stretching region the "B" mode will be more intense than the "A" mode, whereas in the symmetric stretching region the "A" mode will be more intense. For  $\phi = 0^\circ$ , the weaker modes will have zero intensity; at  $\pm 90^\circ$ , the intensities of "A" and "B" modes are predicted to be equal. A twist larger than  $\pm 90^\circ$  is unlikely. Thus in both the antisymmetric and symmetric CH stretching regions of the  $\beta$ -alaninato complexes, we assign the higher frequency mode to the out-of-phase "B" symmetry combination and the lower frequency mode to the in-phase "A" symmetry combination. Assuming equal contribution from the two methylene groups, the relative intensities observed for the symmetric stretching modes, which are better resolved, are consistent with a torsion angle on the order of  $\pm 70^\circ$ . In crystalline  $\Delta$ -*mer*-Co( $\beta$ -ala) $_3$  an average torsion angle  $|\phi| \sim 68^\circ$  was found.<sup>17</sup>

In order to probe the effects of nonequivalent methylene groups, we carried out fixed partial charge (FPC) calculations for an  $ND_2C(1)H_2C(2)H_2C$  fragment with a  $+60^\circ$  NCCC dihedral angle. The CH stretching force constants and CH,CH-gem and CH,CH-trans interaction force constants were adjusted to reproduce the observed frequencies and intensity patterns. Since an amino substituent decreases CH stretching frequencies,<sup>11</sup> the force constant for C(1)H was set lower than that for C(2)H to

(14) Bjerrum, J.; McReynolds, J. P. *Inorg. Synth.* **1946**, *2*, 216.

(15) Yoneda, H.; Yamazaki, S.; Yukimoto, T. In *Stereochemistry of Optically Active Transition Metal Complexes*; Douglas, B. E., Saito, Y., Eds.; American Chemical Society: Washington, DC, 1980; Chapter 16, ACS Symp. Ser. No. 119.

(16) (a) Diem, M.; Gotkin, P. J.; Kupfer, J. M.; Nafie, L. A. *J. Am. Chem. Soc.* **1978**, *100*, 5644. (b) Diem, M.; Photos, E.; Khouri, H.; Nafie, L. A. *J. Am. Chem. Soc.* **1979**, *101*, 6829. (c) Lal, B. B.; Diem, M.; Polavarapu, P. L.; Oboodi, M.; Freedman, T. B.; Nafie, L. A. *J. Am. Chem. Soc.* **1982**, *104*, 3336.

(17) Soling, H. *Acta Chem. Scand.* **1978**, *A32*, 361.

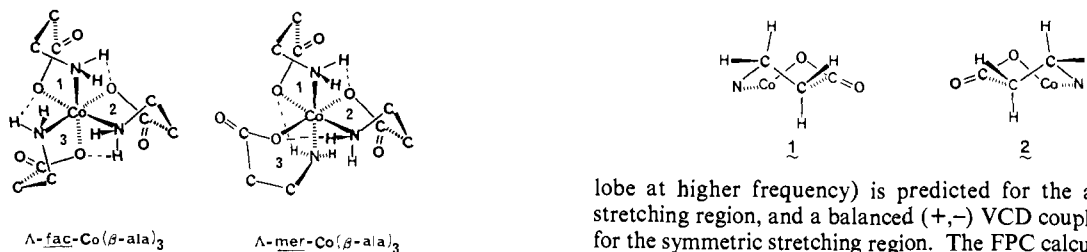


**Figure 3.** Proposed solution structures of  $\Delta$ -*fac*- and  $\Delta$ -*mer*- $\text{Co}(\beta\text{-ala})_3$  showing intramolecular hydrogen bonds between ligands.

account for the mode splitting. The intensity pattern was reproduced only when both the higher frequency antisymmetric and higher frequency symmetric stretches had pseudo "B" symmetry, as assigned in Table I, and in agreement with the degenerate coupled oscillator predictions. The FPC calculations (Table I) predict unbalanced VCD couplets in each region. The calculated modes at 2977 and 2936  $\text{cm}^{-1}$  consist of approximately 30% C(1)H<sub>2</sub> and 70% C(2)H<sub>2</sub> stretching, whereas the modes at 2958 and 2908  $\text{cm}^{-1}$  are  $\sim 70\%$  C(1)H<sub>2</sub> and 30% C(2)H<sub>2</sub> stretching.

### Discussion

In our previous studies of the VCD spectra of metal chelates,<sup>5-7</sup> we proposed ring conformations in solution that are stabilized by ligand–ligand or ligand–counterion hydrogen bonds. In both *mer*- and *fac*- $\text{Co}(\beta\text{-ala})_3$ , interactions between one NH bond of each ligand and a lone pair on the coordinated oxygen of an adjacent ligand are possible. Construction of molecular models suggests that the strongest hydrogen bonds and least steric hindrance in the  $\Delta$ -*fac* and  $\Delta$ -*mer* complexes occurs for the structures depicted in Figure 3. These structures involve the enantiomeric boat conformations 1 and 2 for the  $\beta$ -alaninato rings. We note that the twist of the two methylene groups in 1 or 2 corresponds to the  $\delta$  or  $\lambda$  ring conformations of an ethylenediamine chelate, respectively, and that such structures can readily accommodate a 70° NCCC dihedral angle. In the  $\Delta$ -*fac* complex in Figure 3, all three rings assume conformation 1, whereas in the  $\Delta$ -*mer* complex, rings 1 and 2 have conformation 1 and ring 3 has conformation 2. Alternate torsion angles in the ring that maintain these CH<sub>2</sub>CH<sub>2</sub> twists and the intramolecular hydrogen bonds are also possible.

According to the coupled oscillator mechanism for the CH stretches of the chirally oriented methylene groups in conformation 1, depicted in Figure 2, a balanced (–,+) VCD couplet (negative

lobe at higher frequency) is predicted for the antisymmetric stretching region, and a balanced (+,–) VCD couplet is predicted for the symmetric stretching region. The FPC calculations predict similar but unbalanced couplets. The observation of monosignate VCD bands in each region rules out the CO mechanism as the dominant source of CH stretching VCD intensity for this complex. The frequencies of the VCD bands correspond to the (CH<sub>2</sub>)<sup>asym</sup> "B" and (CH<sub>2</sub>)<sup>sym</sup> "B" stretching vibrations.

In analogy to our interpretation of the monosignate VCD intensity in the CH stretching region of chiral tris(ethylenediamine) complexes,<sup>6</sup> we propose that the monosignate VCD features for  $\beta$ -alaninato ligands are due to ring current enhancement. The mechanism, shown in Figure 4, is an example of empirical Rule 3 governing the sense of vibrationally generated ring currents.<sup>6</sup> In the "B" modes, the equatorial CH bonds are oscillating in an out-of-phase, concerted, push–pull fashion. The contraction of one CH(eq) and elongation of the other is proposed to push electrons along the methylene CC bond in the direction of the concerted CH motion. Due to the closed ring pathway, positive ring current (opposite in direction to electron flow) is initiated around the ring, which results in a magnetic moment. The motion of the axial CH bonds is transverse to the ring plane and does not initiate ring current. The directions of the net electric dipole transition moments,  $\mu$ , and ring current magnetic dipole transitions,  $m$ , are depicted by open arrows in Figure 4 for the "B" and "A" CH stretches of the rings in conformations 1 and 2. For the "A" modes, no ring current is initiated due to the opposing effects of the two equatorial CH bond motions, and VCD intensity, proportional to the rotational strength  $R = \text{Im}(\mu \cdot m)$ , is not predicted to be enhanced for "A" symmetry CH stretches. For the "B" symmetry modes of conformation 1, enhanced positive VCD in the antisymmetric stretching region and enhanced negative VCD in the symmetric stretching region are predicted, in agreement with the observed VCD spectrum of  $\Delta$ -*fac*-( $\beta$ -alaninato)cobalt(III) (Figure 1), for which all three rings are proposed to have conformation 1. Ring current enhanced VCD of the opposite signs are predicted for the enantiomeric conformation 2. In  $\Delta$ -*mer*-( $\beta$ -alaninato)cobalt(III), one ring is proposed to have conformation 2 and two rings conformation 1. Some of the VCD intensity thus

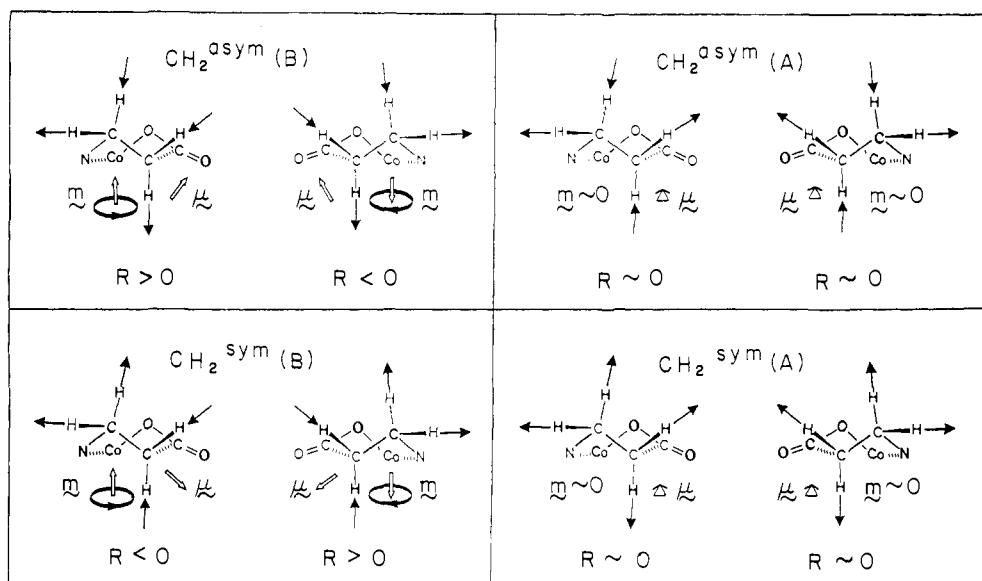


**Figure 4.** Ring current mechanism for enhancement of CH stretching VCD in  $\beta$ -alaninato ligand rings. For each mode, the ring on the left has conformation 1 and the ring on the right has conformation 2. The loop with arrow for each "B" mode shows the direction of positive current around the ligand ring initiated by out-of-phase concerted motion of the equatorial CH bonds. Open arrows give the directions of the ring current magnetic dipole transition moment ( $m$ ) and net electric dipole transition moment ( $\mu$ ) for each mode.

cancels in the *mer* complex. In agreement with this interpretation, the VCD intensities in the CH stretching region of the  $\Lambda$ -*mer* complex, which are lower than those in the  $\Lambda$ -*fac* complex by approximately a factor of 3, correspond in sign and magnitude to that predicted for a single ring in conformation 1.

We note that the negative CH symmetric stretching VCD feature in the spectrum of  $\Lambda$ -*fac*-Co( $\beta$ -ala)<sub>3</sub> has a weak negative shoulder corresponding to the "A" absorption band. This feature may arise from the coupled oscillator mechanism, which is predicted to result in negative VCD for this band (Figure 2 and Table 1), although it is unclear why a similar feature is absent in the spectrum of the  $\Lambda$ -*mer* complex. Other CO features are not evident due to partial cancellation and to the large ring current contributions.

The only crystal structure for these complexes that has been reported is for  $\Delta$ -*mer*-tris( $\beta$ -alaninato)cobalt(III) tetrahydrate.<sup>17</sup> In the crystal, the ligands were found to have a "twist-boat" conformation, with the sense of twist of one ligand opposite to that of the other two. The conformations of the methylenes correspond to two rings with a  $\delta$  twist and one with a  $\lambda$  twist; that is, one ring has an opposite twist compared to our proposed solution structure. In the crystal, hydrogen-bonding interactions between amine hydrogens and oxygen atoms on water or on an adjacent complex stabilize the ring conformations. Closer examination of

the crystal structure data indicates that for two ligands one NH bond lies within hydrogen-bonding distance (2.3–2.6 Å) and orientation of the coordinated oxygen on an adjacent ligand of the same complex. Such interactions are similar to those we propose in Figure 3 for the complex in solution.

### Conclusions

This study of the CH stretching VCD spectra of tris( $\beta$ -alaninato)cobalt(III) complexes has provided further evidence for the ring current mechanism of VCD, since enhanced VCD intensity can be clearly identified with the modes of "B" symmetry. Only in these modes can the CH stretches generate net current around the ligand ring. Even though the frequencies of the "A" and "B" modes are split, there is little evidence of coupled oscillator contributions, due to the large ring current effects. The VCD spectra of both the  $\Lambda$ -*fac* and  $\Lambda$ -*mer* complexes are consistent with solution conformations stabilized by intramolecular hydrogen bonding between ligands.

**Acknowledgment.** We acknowledge financial support by grants from the National Institutes of Health (GM-23567) and the National Science Foundation (CHE 86-02854).

**Registry No.**  $\Lambda$ -*fac*-Co( $\beta$ -ala)<sub>3</sub>, 71425-08-6;  $\Lambda$ -*mer*-Co( $\beta$ -ala)<sub>3</sub>, 71300-67-9.

## Synthesis and Characterization of Novel Flavin-Linked Porphyrins. Mechanism for Flavin-Catalyzed Inter- and Intramolecular 2e/1e Electron-Transfer Reactions<sup>1,2</sup>

Jun Takeda, Shigeru Ohta, and Masaaki Hirobe\*

Contribution from the Faculty of Pharmaceutical Sciences, University of Tokyo, Hongo, Bunkyo-ku, Tokyo 113, Japan. Received December 30, 1986

**Abstract:** The synthesis of several flavin-linked porphyrins is described. The two moieties (Fl<sub>ox</sub>C<sub>n</sub>(TPP)M, M = H<sub>2</sub> and Mn<sup>III</sup>Cl) are covalently linked by an amide linkage with a methylene spacer group [C<sub>n</sub>, n = 1–3] between the ortho position of (*o*-aminophenyl)triphenylporphyrin and the N<sup>3</sup> or N<sup>10</sup> positions of the flavin. The Fl<sub>ox</sub>C<sub>n</sub>(TPP)M (**1a–e**) were characterized by UV-visible, <sup>1</sup>H NMR, and IR spectra. The proximity conformation of the flavin and porphyrin ring was demonstrated by <sup>1</sup>H NMR studies of Fl<sub>ox</sub>C<sub>n</sub>TPPH<sub>2</sub>. The electrochemistry of Fl<sub>ox</sub>C<sub>n</sub>(TPP)M was investigated by cyclic voltammetry and differential-pulse polarography. Cyclic voltammetry demonstrated that the flavin reduction potentials, Fl<sub>ox</sub> + e<sup>-</sup> = Fl<sup>-</sup> and Fl<sup>-</sup> + e<sup>-</sup> = Fl<sup>2-</sup>, were positively shifted by the proximity of the linked porphyrin moiety. Flavin-catalyzed 2e/1e electron-transfer reactions from dihydropyridines to (TPP)Mn<sup>III</sup>Cl have been investigated kinetically in intermolecular systems (PyH<sub>2</sub> + Fl<sub>ox</sub> + (TPP)Mn<sup>III</sup>Cl) as well as in intramolecular systems (PyH<sub>2</sub> + Fl<sub>ox</sub>C<sub>n</sub>(TPP)Mn<sup>III</sup>Cl) in ethanol solution. In intermolecular systems, the presence of flavin enhances the apparent rates of electron transfer significantly. The kinetic behavior of the intermolecular system is zero order with respect to the (TPP)Mn<sup>III</sup>Cl concentration and first order with respect to the PyH<sub>2</sub> and Fl<sub>ox</sub> concentrations, when PyH<sub>2</sub> is in excess and Fl<sub>ox</sub> is used in 0.25–1.5-fold to (TPP)Mn<sup>III</sup>Cl. These observations indicate that the flavin acts as 2e/1e catalyst. In intramolecular systems, the kinetic behavior differs for the various Fl<sub>ox</sub>C<sub>n</sub>(TPP)Mn<sup>III</sup>Cl systems. Whereas Fl<sub>ox</sub>C<sub>1</sub>(TPP)Mn<sup>III</sup>Cl shows clean first order, Fl<sub>ox</sub>C<sub>2</sub>(TPP)Mn<sup>III</sup>Cl and Fl<sub>ox</sub>C<sub>3</sub>(TPP)Mn<sup>III</sup>Cl exhibit a mixed-order behavior. The apparent second-order rate constants are increased for the intramolecular systems. The rate enhancements by the intramolecular effect are as follows:  $k_{\text{intra}}/k_{\text{inter}} = 8.0$  (**1a**), 3.9 (**1b**), 2.1 (**1c**), 1.7 (**1d**), and 1.8 (**1e**). These results show that the  $k_{\text{intra}}/k_{\text{inter}}$  values are affected by the methylene spacer length and the linking position. Possible reasons for the rate enhancement are discussed by using electrochemical data, conformational data, and kinetic isotope effects. The proposed reaction mechanism for the intramolecular system, especially for Fl<sub>ox</sub>C<sub>1</sub>(TPP)Mn<sup>III</sup>Cl, involves a ternary complex such as [PyH<sub>2</sub>...Fl<sub>ox</sub>... (TPP)Mn<sup>III</sup>Cl]. The described systems are relevant models for biological electron-transfer processes requiring flavin 2e/1e catalysis and for flavin-heme interaction as in flavohemoproteins.

Flavin coenzymes are prosthetic groups in a number of redox proteins and catalyze many types of redox reactions including hydrogen-transfer reactions, electron-transfer reactions, and activation of dioxygen.<sup>3,4</sup> Thus, chemical investigations of the flavin

coenzyme have helped considerably in the understanding of enzymatic reaction mechanisms.<sup>4</sup> Unlike the NAD(P)H coenzyme, flavin can readily undergo a one-electron transfer as well as two-electron transfer, since the isoalloxazine ring system has three

(1) Preliminary communication: Takeda, J.; Ohta, S.; Hirobe, M. *Tetrahedron Lett.* **1985**, 26, 4509–4512.

(2) Takeda, J.; Ohta, S.; Hirobe, M. Presented in part at the 8th IUPAC Conference on Physical Organic Chemistry, Tokyo, Aug 24–29, 1986; Abstracts p 175.

(3) (a) Walsh, C. *Acc. Chem. Res.* **1980**, 13, 148–155. (b) Walsh, C. In *Enzymatic Reaction Mechanisms*; Freeman: San Francisco, 1979; pp 358–448.

(4) Bruce, T. C. *Acc. Chem. Res.* **1980**, 13, 256–262, and references therein.